Acknowledgments

I am very grateful for all inspiring help from Predrag Cvitanović which has been important for me, both professionally and personally. I want to thank all the people in the chaos group at the Niels Bohr Institute and Nordita where I have experienced a very good professional and social environment. For interesting discussions here where I learned a lot I thank Vivianne Baladi, Tomas Bohr, Hans Henrik Rugh, Freddy Christiansen, Stephen Creagh, Per Dahlqvist, Peter Dimon, Hans Frisk, Mogens Høgh Jensen, Zoltan Kaufmann, Ronnie Mainieri, Mads Nordahl, Agata Pavone, Gunnar Russberg, Per Rosenqvist, Thomas Schreiber, Gabor Vattay and many others. I want to thank many of the people I have met at a number of conferences and other places for many inspiring discussions. I also would like to thank Jan Frøyland for introducing me to the world of chaos, and to all friends at the physics department in Oslo. I am grateful for the help I got with some of my drawings from Elisabeth Grothe.

I thank NAVF (The Norwegian Research Council) for the grant making this project possible.

I am grateful to Sidsel Hoelsæter for great patience with me moving around all the time, and to my parents, Inger and Ronald Hansen, for all their help and encouragement throughout the years. I will also thank my grandparents, Helmine and Paul Paulsberg, and dedicate this work to the memory of my grandfather.

Introduction

After calculus was invented by Newton and Leibniz 300 years ago, the main goal of mechanics has been to find an analytic solution describing the exact dynamics of a given mechanical system. If an analytic solution could not be obtained, then one tried to find a perturbation solution close to an exact solution. Problems which could not be solved this way were usually left untouched by mathematicians and physicists. Newton obtained the exact solution of the gravitational two body problem while for the three body problem he could obtain only perturbation solutions in some limits. The way we attack these kinds of mechanical problems (and other dynamical problems) from the chaos-theory point of view is different. We try to explain the dynamics not as one analytically describable path, but as a collection of different possible paths from which one can calculate average quantities of the system. The questions we ask and can answer are closer to the theory of statistical mechanics and quantum mechanics than to the traditional mechanics.

The first to emphasize that one should study the global dynamics in the phase space of the system in a qualitative way was Poincaré who introduced several of the ideas and methods we use today. He discussed stable and unstable manifolds, defined the surface of section (today called the Poincaré map), and stressed the importance of the periodic orbits. By the end of the 19th century Poincaré and others proved that the three body problem did not have the analytic solutions which Newton hoped to find. The ideas of Poincaré were developed by other mathematicians in the beginning of the 20th century, but received scant given little attention in physics and applied mathematics. Birkoff continued Poincaré's work on discrete mappings and stable and unstable manifolds. In the middle of this century the digital computer was developed, and use of computers to numerically solve problems which do not have analytic solutions became a very important part of the study of dynamical systems. The interplay between the numerical simulations and development of the theory has been fruitful, with many examples of numerical experiments giving new theoretical insights, such as the Fermi-Pasta-Ulam coupled oscillator chains, the Lorenz attractor, the integrable Toda lattice, the chaotic Hénon-Heile problem, the Feigenbaum period doubling, and the Hénon attractor. These results gave new insights in the structure of the problems without a traditional analytic solution. Important theoretical results were obtained by mathematicians like Kolmogorov, Arnold, Moser, Sinai, Smale, Newhouse, Ruelle and many others. These "strange" problems are now usually referred to as *chaotic systems*. There is no agreement on the ultimate definition of a chaotic system, but this may be unimportant since in practice there is general agreement on what the interesting questions

are. In the last 20 years there has been a huge interest in chaotic systems and many new results have been obtained. The work giving the background for this thesis will be discussed in the text where we use these results. We build on the results concerning symbolic dynamics obtained by Sharkovskii, Smale, Metropolis, Stein, Stein, Milnor, Thurston, Grassberger, Cvitanović and many others.

"Quantum-chaos" is the youngest of the theories in the "chaos family" and at the moment maybe the one with fastest progress. The problem of quantum mechanics and chaos is discussed from many different points of view, all the way from philosophical discussions to the real experiments. The semi-classical theory of chaotic systems is of most interest to us since this theory gives a close relation between the study of a classical system and the corresponding quantum systems, and for both the quantum system and the classical systems description of periodic orbits of the classical system plays an essential role.

In this thesis we will study the structure of orbits in classical chaotic systems and a major tool will be the concept of symbolic dynamics. As much of the work in chaos theory, this work is a mix of theoretical results, computer simulations and applications to physical systems. We do not claim that the theoretical results here are rigorously proven; they are mostly based on numerics and conjectures. Some of the theoretical results may easily be turned into theorems while other conjectures will need a lot of work to be proven, falsified or improved. We have obtained descriptions of the orbits existing in chaotic systems and these descriptions can be used in calculations of quantities like the energy levels of a quantum system. In this thesis we work out a method for obtaining this description. Most applications of this are left as future work.

A number of new results connected to the symbolic description of chaotic systems are presented here. Bifurcation diagrams for three-modal one-dimensional maps are drawn in a symbolic parameter plane, topologically equivalent to a usual parameter plane. A global bifurcation diagram for this map has not been shown before. We obtain similar bifurcation diagrams for the general once-folding two-dimensional maps; the Hénon map is one two-parameter realization of such once-folding map. These bifurcation diagrams are obtained by an approximation procedure which orders the infinite-dimensional parameter space in a hierarchical manner. This yields in a rather complicated description of bifurcations which agrees with numerics for the Hénon map worked out in detail by Mira [153] and with other numerical examples of once-folding maps. We think that this description presented here for the first time is the correct way to describe these bifurcations. There are many questions not yet settled concerning the correctness of the assumptions underlying this theory.

The important question of a unique partition of the folding map is addressed and we propose a method that should yield a unique partition. Generalization of these results to an n-folding two-dimensional map is also discussed. For a number of billiard systems; 3-disk, 4-disk, 7-disk, hyperbola billiard, stadium billiard and wedge billiard, we define a well ordered symbolic dynamics description and obtain a pruning front. The pruning front distinguishes between symbol strings corresponding to the admissible and the forbidden orbits. This can be used to construct an approximate Markov partition. Finding the topological entropy is the simplest application of the theory. These results are the first systematical description of admissible orbits for the billiard systems and this is the first implementation of a construction of approximate Markov partitions in billiard systems. We also investigate in some detail the bifurcation of orbits in billiard systems as the parameters change. This yield singular bifurcations which we show can be described by symbolic dynamics. We compare the singular bifurcations of billiards with bifurcations found in smooth Hamiltonian potentials, and find families of orbits bifurcating together described by the same symbolic dynamics in both systems. This relation between symbolic description of orbits in billiards and in smooth systems, apparantly not investigated before, offers a better understanding of bifurcation of orbits in smooth Hamiltonian systems.

The pruning front for dispersive billiards and some of the results for bifurcations in billiards and smooth potentials are published in refs. [108, 109, 110]. One result concerning the change of symbolic description of unstable orbits in the Hénon map is also published in ref. [107].

Part I

One-dimensional maps

Chapter 1

Unimodal map

1.1 Bifurcations in the unimodal map

A curious feature of chaotic systems is that the description of most phenomena observed in many different chaotic systems is greatly aided by a proper understanding of the simple one-dimensional unimodal map, so we will devote a considerable amount of space to the review of this well known and much studied map.

A unimodal map is a continuous one-dimensional function $\mathbb{R} \to \mathbb{R}$ with a monotonously increasing (or decreasing) branch, a critical point x_c as the maximum (minimum) point, and a monotonously decreasing (respectively increasing) branch. We assume in this section that the critical point is a maximum point. The dynamics of the point x is given by the iteration

$$x_{t+1} = f(x_t, a) \tag{1.1}$$

and some simple examples of unimodal maps are the logistic map

$$x_{t+1} = a x_t (1 - x_t) \tag{1.2}$$

drawn in figure 1.1 for $a = 3.92$ and the tent map

$$x_{t+1} = \begin{cases} a x_t & x_t \leq 1/2 \\ a(1 - x_t) & x_t > 1/2 \end{cases} . \tag{1.3}$$

drawn in figure 1.2 for $a = 1.75$. For convenience we assume $a \geq 0$, because $a < 0$ gives a function with a minimum point and with the same dynamics. Both the logistic map and the tent map are unimodal and have similar topological properties, while metric properties are very different. The tent map is a singular map, while the logistic map is typical for smooth maps with a critical point $f'(x_c) = 0$ with

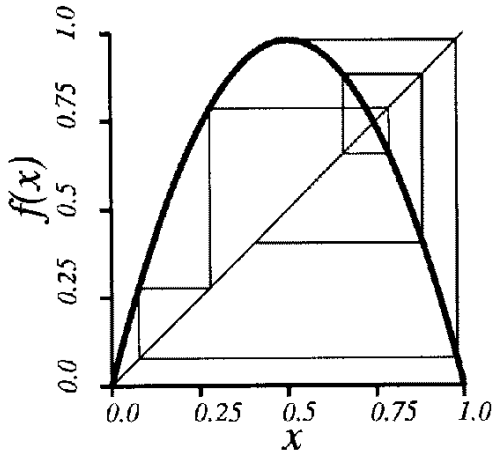

Figure 1.1: The logistic map $f(x) = ax(1-x)$ with $a = 3.92$ and the orbit starting at the point $x = 0.5$.

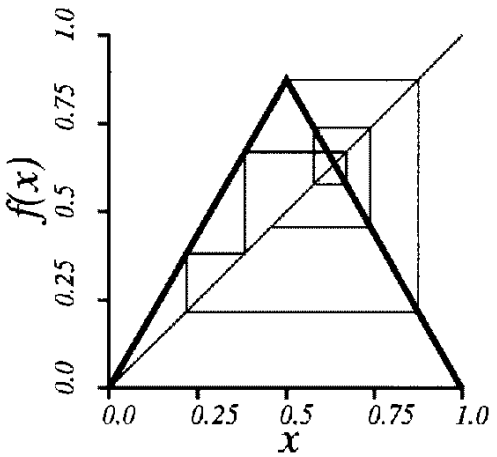

Figure 1.2: The tent map $f(x) = ax$ if $x \leq 0.5$ and $f(x) = a(1-x)$ if $x > 0.5$ and the orbit starting at the point $x = 0.5$.

$f''(x_c) \neq 0$. We will find that two-dimensional systems often have bifurcations similar to those we find in one of these two simple maps.

The iteration of points x is illustrated graphically in the figures 1.1 and 1.2. We draw a horizontal line from the point $x = x_t$ on the function f to a point on the diagonal $y = x$ and then we draw a vertical line from this point on the diagonal to a point on the function f. This point has $x = x_{t+1}$ and we find the time series

$$x_1 x_2 x_3 \ldots \tag{1.4}$$

from the starting point x_0. It is this time series we want to study – its convergence to an asymptotic attractor and the transient dynamics.

The first numerical experiment we do on the computer is to find the attractor $\lim_{t\to\infty} x_t$ and plot the attractor as a function of the parameter a. This picture is the well known bifurcation tree for the logistic map in figure 1.3 [144, 72]. The tent map also has an attractor, and the bifurcation tree for the tent map is drawn in figure 1.4.

The symbolic sequence of an orbit given by the time series (1.4) is defined as follows. In a smooth map the critical point x_c is the x-value giving $f'(x) = 0$ and for the logistic map $x_c = 1/2$. The tent map has a special point which we also may call a critical point at $x_c = 1/2$ where $f(x)$ has a maximum point and $f'(x)$ is discontinuous. Let [152] the binary symbols be defined as

$$s_t = \begin{cases} 1 & \text{if } x_t > x_c \\ 0 & \text{if } x_t < x_c \end{cases} . \tag{1.5}$$

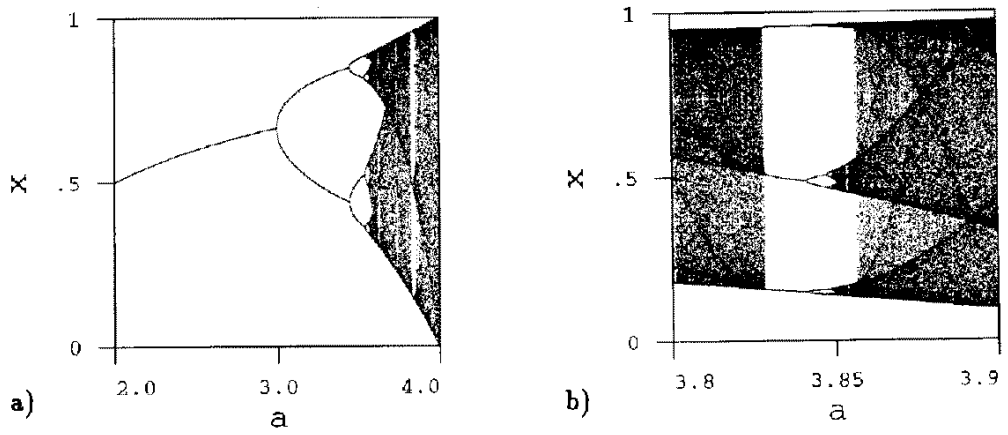

Figure 1.3: The bifurcation tree of the logistic map. a) The whole tree, b) magnification around the period 3 resonance.

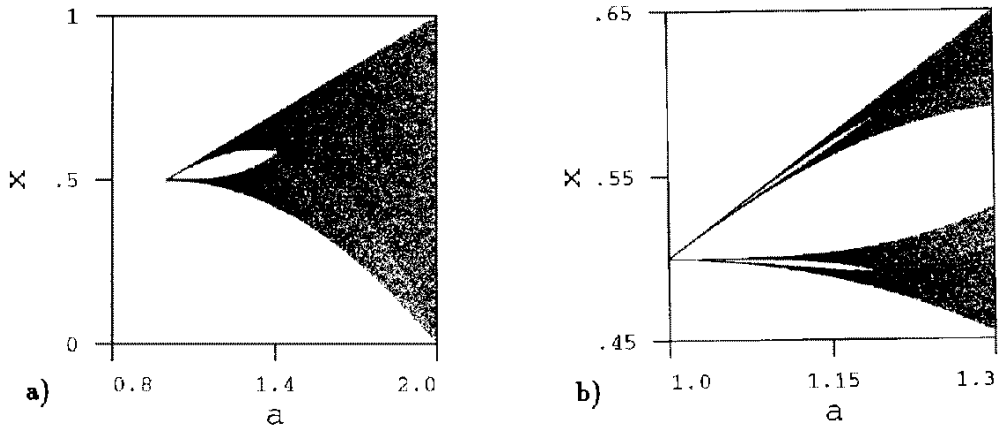

Figure 1.4: The bifurcation tree of the tent map. b) magnification around the creation of the fixed point.

The symbol string $S = s_1 s_2 s_3 \ldots$ with $s_t \in \{0, 1\}$ is the *forward itinerary* of point x_0. Symbols L and R are often used [147] instead of 0 and 1 so the symbols indicate if the point x_t is on the left side (L) or the right side (R) of the critical point. If $x_t = x_c$ the symbol $s_t = C$ is often used but we will investigate separately these special orbit.

Figure 1.1 shows the trajectory of the point $x_0 = x_c = 0.5$ in the logistic map and we read the symbol sequence from the figure

$$s_1 s_2 s_3 s_4 s_5 s_6 \ldots = 100111 \ldots \tag{1.6}$$

The tent map in figure 1.2 gives the same first 6 symbols when we start with $x_0 = x_c = 0.5$. The symbol string obtained by choosing $x_0 = x_c$ is of special interest and this string is called the kneading sequence of the unimodal map.

A periodic orbit of length n is a real solution of

$$f^{(n)}(x) = f(f(\ldots f(x)\ldots)) = x \tag{1.7}$$

The unimodal map, eq. (1.7), has 2^n solutions in the complex plane, and we will therefore have 2^n or less period n orbits for the map.

A periodic orbit of length n is described by an infinite repetition of a length n symbol string, indicated by the line over the string:

$$\overline{S} = (s_1 s_2 s_3 \ldots s_n)^\infty = \overline{s_1 s_2 s_3 \ldots s_n} \tag{1.8}$$

Each point x_t in a periodic orbit can be associated with one of the 2^n possible symbolic strings $\overline{s_1 s_2 \ldots s_n}$. A cyclic permutation of the symbolic string $\overline{s_1 s_2 \ldots s_n}$ to a new string $\overline{s_k s_{k+1} \ldots s_n s_1 \ldots s_{k-1}}$ is the description of the point x_{t+k-1} in the same periodic orbit.

A periodic orbit is stable if

$$\left| \frac{df^{(n)}(x)}{dx} \right| = |f'(x) \cdot f'(f(x)) \cdot \ldots \cdot f'(f(f(\ldots f(x)\ldots)))| < 1 \tag{1.9}$$

If we draw the function $f^{(n)}(x)$ then for a stable periodic orbit the slope of this function at the fixed point is between -1 and 1. The interval on the parameter axis where a periodic orbit is stable is called the stable window of the periodic orbit.

1.1.1 Fixed point and period doubling

Both fixed points (period 1 orbits) $x = 0$, $x = 1 - 1/a$ of the logistic map (1.2) exist for all $a > 0$. The first solution $x = 0$ is stable for $0 < a < 1$ and unstable for $a > 1$. This solution has $x < x_c$ for all parameter values and we denote this orbit

as $\overline{0}$ and the point as $x_{\overline{0}}$ where the index gives the symbolic description of the orbit. To avoid a too cumbersome notation we don't use the line over the symbols if it is clear from the context that we refer to a periodic orbit. We then write x_0 and 0 which should be understood as $x_{\overline{0}}$ and $\overline{0}$.

The other fixed point $x = 1 - 1/a$ is unstable for $0 < a < 1$, stable for $1 < a < 3$ and unstable for $a > 3$. This fixed point has $x < x_c$ for $0 < a < 2$ and $x > x_c$ for $a > 2$. As the interesting dynamics take place for $a > 2$ it is tempting to identify this orbit by $\overline{1}$ and denote the point $x_{\overline{1}}$ for all values of the parameter a, but this has to be done with care. It is typical that a stable orbit change symbolic description somewhere within the stable window. In one-dimensional smooth maps this is always at the parameter value where the orbit is super-stable $df^{(n)}(x)/dx = 0$, i.e. where one of the points in the orbit is identical to x_c. In a unimodal map there is only one of the n points in a period n orbit that can cross the critical point and the symbolic description of the orbit can only change in one symbol

$$\overline{s_1 s_2 \dots s_{n-1} s_n} \to \overline{s_1 s_2 \dots s_{n-1}(1 - s_n)} \tag{1.10}$$

In the multimodal maps discussed in chapter 2 there are several points in the periodic orbit that can cross a critical point and the symbolic description can change in different ways. We choose to call this second fixed point $\overline{1}$ but we should always remember that when an orbit is stable , its symbolic dynamics may change and is not unique. In the unimodal map an unstable orbit has a unique symbolic description.

The stability of the fixed point $\overline{1}$ changes from $f'(x_{\overline{1}}) = 1$ at $a = 1$ to $f'(x_{\overline{1}}) = 0$ at $a = 2$ and to $f'(x_{\overline{1}}) = -1$ at $a = 3$. When $f'(x_{\overline{1}}) < 0$ the fixed point has the unique symbolic description $\overline{1}$. The interval $a \in (1, 3)$ is the stable window for the fixed point.

The tent map has a fixed point $x_0 = 0$ for all $a > 0$ and a fixed point $x_1 = a/(a + 1)$ that exists for $a > 1$ and this fixed point is unstable for all $a > 1$. The fixed point x_1 does not have any stable window such as the fixed point in the logistic map and the fixed point is uniquely described by the symbolic description $\overline{1}$.

At $a = 3$ the fixed point x_1 of the logistic map has a period doubling bifurcation where the fixed point becomes unstable and a period 2 orbit

$$x_{01} = \frac{a+1}{2a} + \frac{1}{2a}\sqrt{(a+1)(a-3)} \tag{1.11}$$

$$x_{10} = \frac{a+1}{2a} - \frac{1}{2a}\sqrt{(a+1)(a-3)} \tag{1.12}$$

is created and exists for all $a > 3$. The stability $df^{(2)}(x)/dx$ is 1 at $a = 3$, it is 0 at $a = 1 + \sqrt{5} \approx 3.2361$ and it is -1 at $a = 1 + \sqrt{6} \approx 3.4495$. For larger values of a the orbit is unstable. Close to the bifurcation point at $a = 3$ both points in the

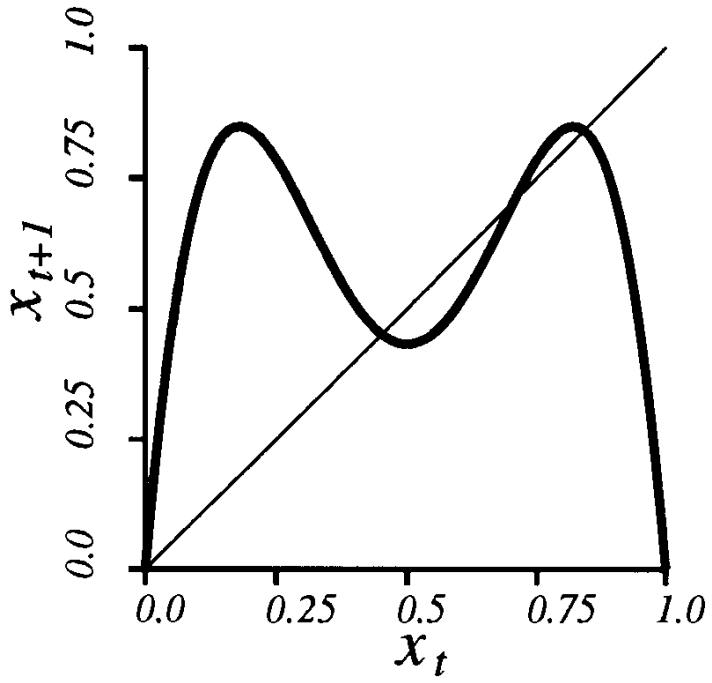

Figure 1.5: The second iterated function $f^{(2)}(x)$ for $a = 3.4$. The four fixed points of this function is the two fixed point $\overline{0}$ and $\overline{1}$ and the two points in the orbit $\overline{10}$.

period 2 orbit are close to the fixed point on the right side of x_c, but for $a > 1-\sqrt{5}$ there is one point on each side of x_c. We denote the orbit by $\overline{10}$ and its points $x_{\overline{01}}$ and $x_{\overline{10}}$ ($x_{\overline{01}} > x_{\overline{10}}$). In figure 1.5 the function $f^{(2)}(x)$ is drawn and the period 2 orbit appears as two fixed points in this drawing.

At $a = 1+\sqrt{6}$ the period 2 orbit becomes unstable and a period 4 orbit is born. After this orbit has passed the super-stable point its symbolic description is $\overline{1011}$ with the four points $x_{\overline{1110}} < x_{\overline{1011}} < x_{\overline{1101}} < x_{\overline{0111}}$. Notice that the map of one of this points give another of the points where the index is a cyclic permutation of the symbolic string $x_{\overline{0111}} = f(x_{\overline{1011}})$, $x_{\overline{1110}} = f(x_{\overline{0111}})$, $x_{\overline{1101}} = f(x_{\overline{1110}})$ and $x_{\overline{1011}} = f(x_{\overline{1101}})$.

We can generalize the period doubling bifurcations. Each periodic orbit bifurcates into an orbit with twice the length and for one parameter value $a_\infty = 3.5714\ldots$ there is an accumulation point where the length of the orbit goes to infinity. It has been shown by Feigenbaum [72, 73, 74] that there is a universal scaling law for all maps which have a quadratic critical point. The universality follows from the Cvitanović–Feigenbaum functional equation $g(x) = -\alpha g(g(-x/\alpha))$.

The symbolic description of the period doubling orbits is given by Metropolis, Stein and Stein (MSS) [147]. The symbolic description of the new orbit is obtained

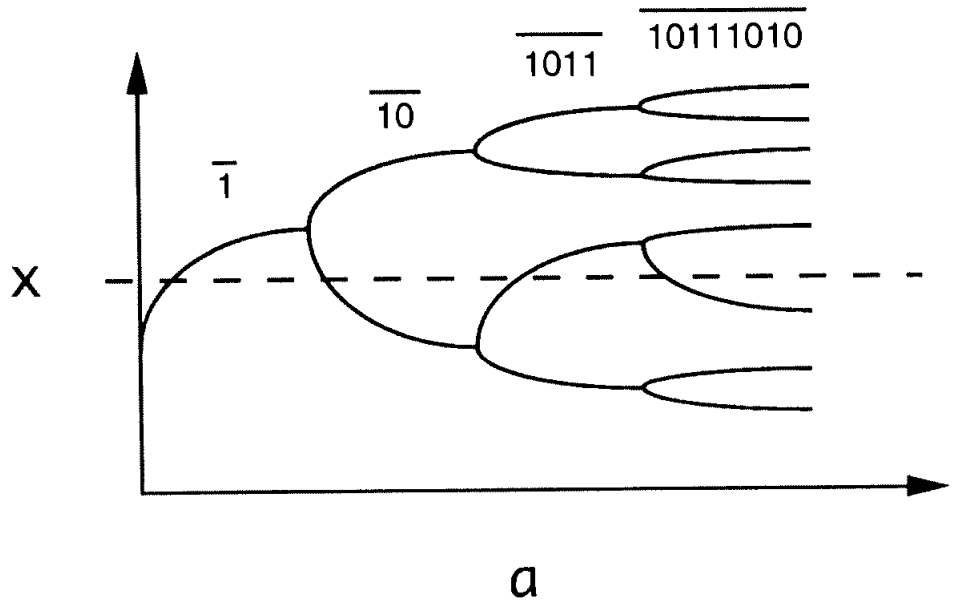

Figure 1.6: The bifurcations of the fixed point and the symbolic description of the periodic orbits.

by writing the old symbol sequence twice and changing the last symbol:

$$\overline{s_1 s_2 \dots s_n} \to \overline{s_1 s_2 \dots s_n s_1 s_2 \dots s_{n-1}(1-s_n)} \tag{1.13}$$

which is called a harmonic by MSS. The period 4 orbit $\overline{1011}$ bifurcates to the period 8 orbit $\overline{10111010}$ etc. Figure 1.6 shows the bifurcation of the fixed point and the symbolic description of the orbits. We should also observe that the number of symbols 1 in these symbol strings is always odd because only orbits with an odd number of 1s can have stability -1 and become unstable in a period doubling bifurcation.

At a parameter $a < a_\infty$ the attractor is a period n orbit and the repellor is the union of shorter unstable periodic orbits. A point x is a *non-wandering point* if for any neighborhood U of x there is a time t such that $U \cap f^{(t)}(U) \neq \emptyset$. The union of all non-wandering points are the *non-wandering set* of the map. For such a parameter the non-wandering set is the union of the periodic orbits.

The periodic orbits have preimages on the x-axis. In figure 1.7 the preimages of the stable fixed point $\overline{1}$ are drawn as a function of the parameter a. For $a < 2$ there is one preimage of the fixed point while for $a > 2$ there is a infinite number of preimages. In figure 1.8 the preimages of the fixed point are drawn as horizontal lines in the (x_t, x_{t+1}) plane. The preimages converge geometrically to the fixed point $x_0 = 0$ and its preimage $x = 1$.

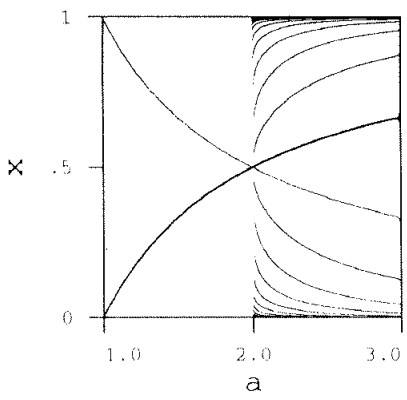

Figure 1.7: The stable fixed point $\overline{1}$ and its preimages as a function of the parameter for $1 < a < 3$.

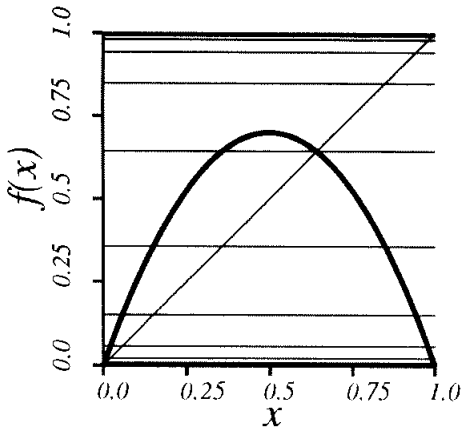

Figure 1.8: The preimages of the stable fixed point $\overline{1}$ drawn as horizontal lines in the (x_t, x_{t+1}) plane. $a = 2.8$

A complete description of the dynamics of the map in the symbolic dynamics language requires a description of both the repellor and the attractor. This can be done by the graphs in figure 1.9 a), b) and c) which gives the symbolic future of any point in the case of the stable orbits $\overline{1}$, $\overline{10}$ and $\overline{1011}$. Moving along a solid curve in the graph corresponds to a symbol 1, while a dashed curve corresponds to a symbol 0. The arrow shows in which direction to move. In figure 1.9 a) we see that there can be an arbitrary number of symbols 0 but after a symbol 1 there can only be symbols 1. For example, the sequence $0001111111\ldots$ is legal but the sequence $0001110111\ldots$ can not exist in the map for this parameter value. This is the description of the symbolic future $s_1 s_2 s_3 \ldots$ and is valid for all starting points, even if $x_0 > x_c$ ($s_0 = 1$).

The graphs are representations of Markov matrixes describing the dynamics in terms of symbols. The graph in figure 1.9 a) represents the matrix

$$\begin{array}{c} \\ 0 \\ 1 \end{array} \begin{array}{c} \begin{array}{cc} 0 & 1 \end{array} \\ \left[\begin{array}{cc} 1 & 1 \\ 0 & 1 \end{array}\right] \end{array} \tag{1.14}$$

The rows are the symbol s_t and the columns are the symbol s_{t+1}. A number 1 in the matrix shows that the string $s_t s_{t+1}$ is legal and a 0 shows that the string $s_t s_{t+1}$ is forbidden.

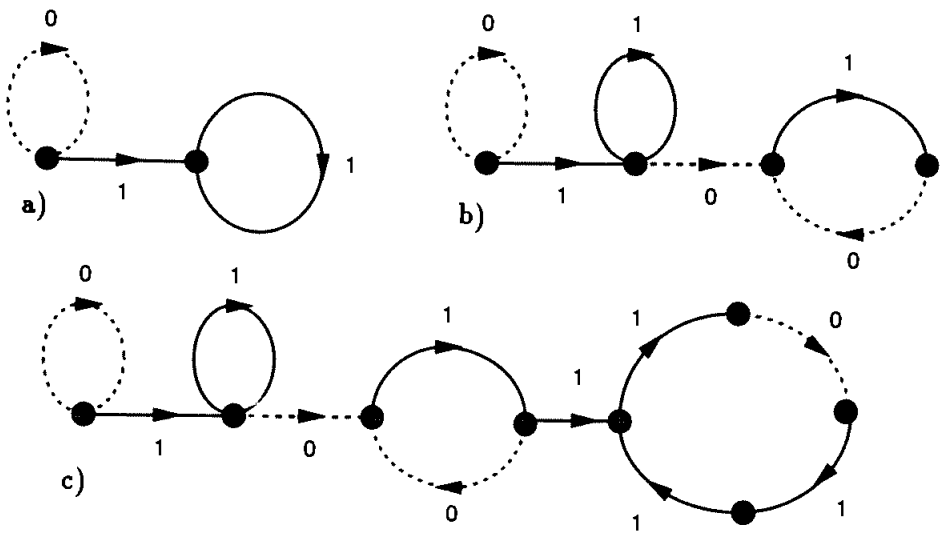

Figure 1.9: Graph representation of legal orbits for a parameter value that gives a stable a) fixed point $\overline{1}$, b) period 2 orbit $\overline{10}$, c) period 4 orbit $\overline{1011}$.

The graph in figure 1.9 b) represents the matrix

$$\begin{array}{c} \\ 000 \\ 011 \\ 111 \\ 001 \\ 110 \\ 010 \\ 101 \end{array} \begin{array}{c} \begin{array}{ccccccc} 000 & 011 & 111 & 001 & 110 & 010 & 101 \end{array} \\ \left[\begin{array}{ccccccc} 1 & 0 & 0 & 1 & 0 & 0 & 0 \\ 0 & 0 & 1 & 0 & 1 & 0 & 0 \\ 0 & 0 & 1 & 0 & 1 & 0 & 0 \\ 0 & 1 & 0 & 0 & 0 & 1 & 0 \\ 0 & 0 & 0 & 0 & 0 & 0 & 1 \\ 0 & 0 & 0 & 0 & 0 & 0 & 1 \\ 0 & 0 & 0 & 0 & 0 & 1 & 0 \end{array}\right] \end{array} \tag{1.15}$$

A row in this matrix is a 3 symbol string $s_{t-2}s_{t-1}s_t$ and a column is a 3 symbol string $s_{t-1}s_ts_{t+1}$. A number 0 in the corresponding matrix element means that the combination giving the 4 symbol string $s_{t-2}s_{t-1}s_ts_{t+1}$ is illegal. The graph representation is much simpler and intuitively understandable that the full matrix. We show later than the construction of a graph is relatively simple and in addition it is simple to find the characteristic polynomial of the matrix from the graph representation [40]. In the ζ-function formalism in chapter 11 this is shown to be useful.

If there exists a finite graph there also exists a corresponding finite Markov matrix and a finite Markov partition of the non-wandering set. A system with a finite Markov partition is a system with finite memory in the sense that we only have to know a finite length symbol string of the past to know which choices we

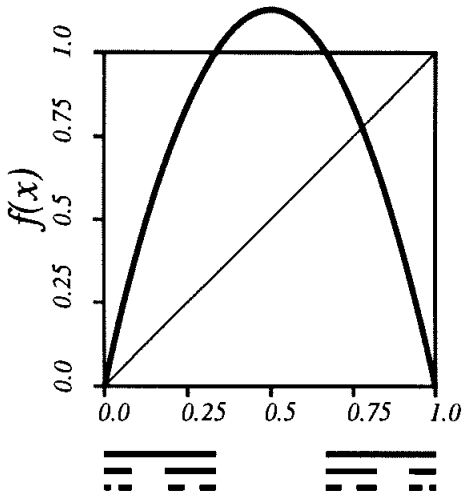

Figure 1.10: The logistic map with $a = 4.5$ and the remaining intervals after 1, 2 and 3 iterations.

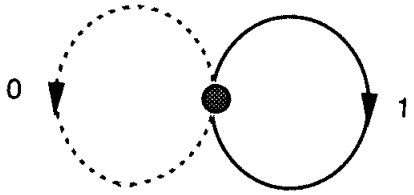

Figure 1.11: The symbolic graph for the complete Cantor set repellor and the attractor for $a = 4$, where all symbol sequences are legal.

have for the next symbol. It is shown by Grassberger [90] that the size of the symbolic graph goes to infinity as we converge to the accumulation point a_∞ of the period doubling bifurcations. At this point the system has infinite memory as defined above.

The tent map has a singular bifurcation for $a = 1$ where all period doubled orbits from the fixed point $\overline{1}$ start to exist and are unstable. The parameter $a = 1$ is then simultaneously the point where the fixed point is borne and the accumulation point a_∞ for the bifurcations of the fixed point.

1.1.2 Unimodal map with complete grammar

If the parameter in the logistic map is $a > 4$ then the critical point x_c diverges for $t \to \infty$ and $x = -\infty$ is the attractor. We will now describe the corresponding repellor. The repellor is a Cantor set and figure 1.10 shows that if we start with the unit interval $(0, 1)$ then at each iteration the middle segment of the remaining intervals escapes from the unit interval.

In symbolic dynamics the orbits in the repellor can be described by all possible combinations of the symbols 0 and 1. The symbols 0 and 1 are letters in a alphabet

$$\{0, 1\} \tag{1.16}$$

and the grammar for a string made from this alphabet is simply that any combination of letters gives a legal string. This grammar is given by the simple graph in

figure 1.11 which represents the Markov matrix

$$\begin{array}{c} \\ 0 \\ 1 \end{array} \begin{array}{c} \begin{array}{cc} 0 & 1 \end{array} \\ \left[\begin{array}{cc} 1 & 1 \\ 1 & 1 \end{array} \right] \end{array} \tag{1.17}$$

If $a = 4$ for the logistic map, x_c is mapped to the fixed point x_0 and we have a chaotic attractor. The symbolic description of the orbits in the attractor is the same complete binary alphabet as for the repellor.

The tent map for $a > 2$ also has a repellor that is described by the same binary symbolic alphabet and for $a = 2$ there is a chaotic attractor with the same description.

1.1.3 The symbolic interval and the kneading sequence

The description of the dynamics for the logistic map when $a_\infty < a < 4$ is complicated and the symbolic description is useful in describing these bifurcations. To make a simple theory for the bifurcations we redefine the symbolic description. The Cantor set in figure 1.10 can be mapped onto the real interval $[0, 1]$ by associating a real number, τ to each infinite symbolic sequence. To keep the ordering of the points on the x-axis we have to define new *well–ordered* symbols w_t.

An increasing function ($f'(x_t) > 0$) preserves the ordering between two points on the x-axis such that if $\hat{x}_t > x_t$ then $\hat{x}_{t+1} > x_{t+1}$. A decreasing function ($f'(x_t) < 0$) reverses the ordering; if $\hat{x}_t > x_t$ then $\hat{x}_{t+1} < x_{t+1}$. The symbol s_t as defined in (1.5) is 0 if the function increases and 1 if the function decreases. We associate with x_t a binary number $\tau(x_t) \in [0, 1]$ as follows

$$\begin{aligned} w_1 &= s_1 \\ w_{t+1} &= \begin{cases} w_t & \text{if } s_t = 0 \\ 1 - w_t & \text{if } s_t = 1 \end{cases} \\ \tau &= 0.w_1 w_2 w_3 \ldots = \sum_{t=1}^{\infty} \frac{w_t}{2^t}. \end{aligned} \tag{1.18}$$

The number $\tau(x_t)$ preserves the ordering of x_t in the sense that if $\hat{x}_{t+1} > x_{t+1}$ then $\tau(\hat{x}_t) > \tau(x_t)$. We call the symbols $w + t$ the well–ordered symbols and $\tau(x_t)$ the well–ordered symbolic future value of x_t or for brevity; the symbolic value.

As long as $a \geq 4$ for the logistic map any real number $0 < \tau < 1$ corresponds to a symbolic description of an orbit in the non-wandering set of the map. If $a < 4$ there is only a subset of the points in the interval $\tau \in [0, 1]$ of the interval that corresponds to the symbolic description of an orbit and the forbidden symbolic values can be

found using the following observation [152]. The largest possible x_t value (except a starting point x_0) is the image of the critical point $x_{\max} = f(x_c)$. An orbit described by a symbolic sequence S will have a point $x > f(x_c)$ if $\tau(S) > \tau(x_c)$ and cannot be an admissible orbit. We define

$$\kappa = \tau(x_c) \tag{1.19}$$

to be the *kneading value* [152] of the unimodal map and the interval

$$(\kappa, 1] \tag{1.20}$$

its *primary pruned interval.*

For the symbolic sequence S, the dynamics is a shift operation

$$S(f^k(x_0)) = \sigma^k S = \{s_{k+1}s_{k+2}s_{k+3}\ldots\} \tag{1.21}$$

and the orbit S is not admissible if τ of any shifted sequence of S falls into the primary pruned interval. For any orbit S there exists a supremum value $\tau^{\max}$ of the orbit and its images

$$\tau^{\max}(S) = \sup_k \tau(\sigma^k S) \tag{1.22}$$

From this it follows

Theorem 1[175, 147, 99, 152]: Let κ be the kneading value of the critical point as defined in (1.19) and $\tau^{\max}(S)$ be the supremum symbolic value of the orbit S as defined in (1.22). Then the orbit S is admissible if and only if $\tau^{\max}(S) \leq \kappa$.

1.1.4 Bifurcations and symbolic parameter space

We can make use of the kneading value when describing the bifurcations in the unimodal map.

The kneading value κ can be considered as a new topological parameter of the map. In figures 1.12 and 1.13 the value of κ is drawn as a function of a for the logistic map and the tent map. The plot is a staircase-like monotone increasing function. The jumps in κ correspond to symbolic values that are not allowed. Each jump in κ has a one to one correspondence to one window on the parameter axis with a stable periodic orbit for the smooth unimodal map. We can consider the kneading interval $\kappa \in [0, 1]$ to be a parameter space for the unimodal map and we will denote κ the symbolic parameter value when we take this point of view.

The tent map has larger jumps in κ in figure 1.13 than in the logistic map because the tent map does not have any windows, but if these two maps have the same kneading value then the same orbits exist for the parameter values a.

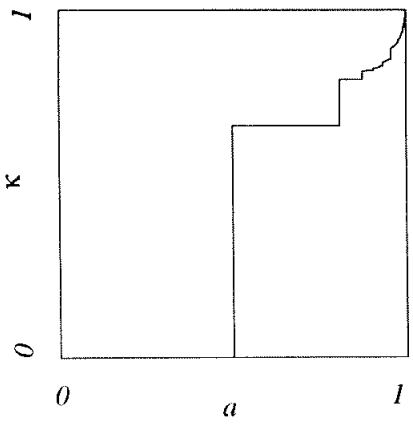

Figure 1.12: The kneading value κ as a function of the parameter a for the logistic map.

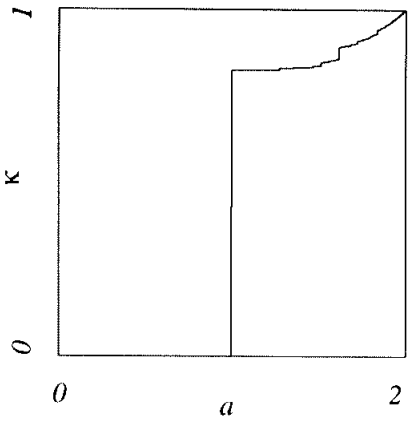

Figure 1.13: The kneading value κ as a function of the parameter a for the tent map.

1.1.5 Band merging bifurcations

One bifurcation in figure 1.3 is the *band merging* bifurcation where $n \cdot 2^{m+1}$ of chaotic bands merge into $n \cdot 2^m$ of chaotic bands. Between two chaotic bands there is an unstable period $n \cdot 2^m$ orbit with $df^{(n)}/dx < -1$ which is an isolated part of the repellor. At the band merging bifurcation this points starts to belong to the attractor when two and two of the $n \cdot 2^{m+1}$ bands join each other at the $n \cdot 2^m$ points of the periodic orbit. The boundaries of the chaotic bands are images of the critical point and the kneading sequence is preperiodic to the symbolic description of the unstable period n orbit.

The simplest example of a band merging bifurcation is the point where two bands merge into one band and the joining point is the fixed point $\overline{1}$. The kneading sequence is here

$$K = 10\overline{1}$$

giving the kneading value

$$\kappa = 0.1\overline{10} = 0.11010101010\ldots = 5/6 \tag{1.23}$$

which is the symbolic parameter value for the two band merging bifurcation for all unimodal maps. No orbits with $\tau^{\max}(S) > 0.1\overline{10}$ exist for this parameter value. In the logistic map the parameter value $a = 3.6785\ldots$ gives this band merging bifurcation and in figure 1.14 the map and the preimages of the fixed point is drawn showing that at this point the parabola is tangent to the closest of the

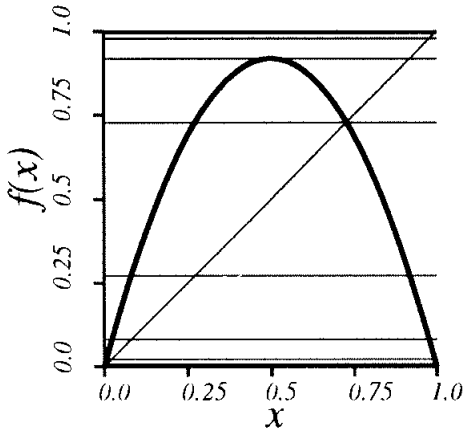

Figure 1.14: The logistic map at the band merging point when two bands merge to one band $a = 3.6785$ and the preimages of the fixed point drawn as horizontal lines.

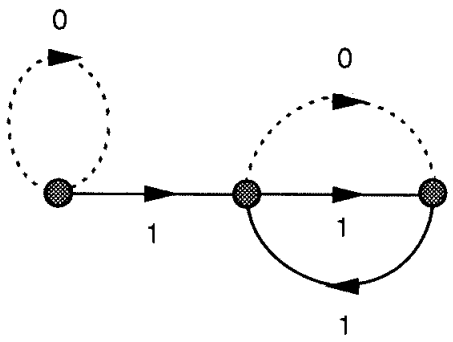

Figure 1.15: The symbolic graph for the band merging point $\kappa = 0.1\overline{10}$.

horizontal lines. There exists a finite grammar describing the non-wandering set and the Markov graph in figure 1.15 shows the rules giving the admissible symbol strings. Comparing with the graphs in figure 1.9 b) and c) we find that the fixed point $\overline{1}$ that used to be a transient orbit now is included in the last, attracting part of the graph. The attractor part of the Markov graph in figure 1.15 can be described by the new two letter alphabet

$$\{01, 11\}$$

All combinations of the two letters 01 and 11 give a symbol string which corresponds to an orbit in the chaotic attractor.

To each period doubling bifurcation there is a corresponding band merging bifurcation. The kneading sequence at a period doubling bifurcation is given by (1.13) and is

$$K = \overline{s_1 s_2 \dots s_n} \rightarrow K = \overline{s_1 s_2 \dots s_n s_1 s_2 \dots s_{n-1}(1 - s_n)} \tag{1.24}$$

The band merging bifurcation which corresponds to this is located at the the kneading sequence

$$K = s_1 s_2 \dots s_n s_1 s_2 \dots s_{n-1}(1 - s_n)\overline{s_1 s_2 \dots s_n} \tag{1.25}$$

with the same symbol string $s_1 s_2 \dots s_n$. The band merging bifurcations for the fixed point in the logistic map also converge to the accumulation parameter a_∞ with the same Feigenbaum scaling factor but with $a > a_\infty$.

The two kinds of bifurcations have the same kneading sequence at the accumulation point:

$$1011101010111011\ldots$$

and this gives the topological parameter value

$$\kappa_\infty = 0.1101001100101101\ldots \tag{1.26}$$

There are similarities between the period doubling and the band merging bifurcation but there are also important differences. The period doubling bifurcation is a local bifurcation depending only on the stability of one orbit. The band merging bifurcation is a global bifurcation involving the critical point and a large non-wandering set. We find that in the discussion of the two dimensional maps in chapter 5 this is analogue to a creation of a homoclinic tangency. Also the similar scaling property of the two kind of bifurcations that exists for the logistic map is not true for all unimodal maps. The tent map has a singular creation of periodic orbits but figure 1.4 shows that there are band merging bifurcations converging to $a_\infty = 1$. The description of the allowed symbol strings changes very differently around the two different bifurcations. The period doubling bifurcations create a new structure in the Markov graph which is a new attractor, leaving the old attractor as a transient loop. The Markov graph does not change from one period doubling bifurcation to the next. The Markov graph for the band merging bifurcation is valid only for this parameter value.

1.1.6 Resonances

In a chaotic band there are resonances where new orbits are created and there is a window with a stable orbit that goes through period doublings and band merging bifurcations and finally in a crisis bifurcation again gives a band attractor. We look in some detail at the simplest of these resonances which is the period 3 resonance in figure 1.3 b).

One stable and one unstable period 3 orbit are created at a tangent bifurcation in the logistic map at $a = 3.8284\ldots$. The symbolic description of both the two orbits are $S = \overline{101}$ at the parameter where they are created. At the super-stable point $a = 3.8319\ldots$ the stable orbit changes symbolic dynamics to $S = \overline{100}$. The symbolic parameter value of the bifurcation creating the two orbits is

$$\kappa = \tau^{\max}(\overline{101}) = 0.\overline{110} = 6/7 \tag{1.27}$$

The symbolic parameter value where the stable orbit crosses the super-stable point is

$$\kappa = \tau^{\max}(\overline{100}) = 0.\overline{111000} = 8/9. \tag{1.28}$$

The orbit $\overline{100}$ undergoes period doubling bifurcations to orbits with a symbolic description given by eq. (1.24) with the initial string $s_1 s_2 s_3 = 100$ and also band merging bifurcations with the kneading sequence given by eq. (1.25).

The *crisis* bifurcation of the period 3 resonance is the parameter value where the attractor changes from 3 chaotic bands to one chaotic band. This is the bifurcation when the critical point maps into the unstable period 3 orbit $\overline{101}$ which for the logistic map occurs for $a = 3.8568\ldots$. This bifurcation has the kneading sequence $100\overline{101}$ and the symbolic parameter value

$$\kappa = 0.111\overline{001} = 25/28. \tag{1.29}$$

In the general description of a resonance two orbits $\overline{s_1 s_2 \ldots s_n}$ and $\overline{s_1 s_2 \ldots s_{n-1}(1-s_n)}$ are born at a tangent bifurcation at the the symbolic parameter value

$$\kappa = \tau(\overline{s_1 s_2 \ldots s_{n-1}(1-s_n)}). \tag{1.30}$$

The string $s_1 s_2 \ldots s_n$ giving a resonance can not be of the form $s_1 s_2 (1 - s_{(n/2)}) s_1 s_2 \ldots s_{(n/2)}$ since this orbit would be born at a period doubling, the number of symbols '1' in $s_1 s_2 \ldots s_n$ is odd and the cyclic permutation $(\overline{s_1 s_2 \ldots s_n})$ is the permutation giving the largest value of τ. The resonance has period doubling and band merging bifurcations with $\overline{s_1 s_2 \ldots s_n}$ as the generating string and the crisis bifurcation takes place at

$$\kappa = \tau^{\max}(s_1 s_2 \ldots s_n \overline{s_1 s_2 \ldots s_{n-1}(1-s_n)}). \tag{1.31}$$

The ordering of resonances along the parameter axis follows the size of $\tau^{\max}(S)$ and this ordering of orbits is often called the MSS (Metropolis, Stein, Stein) sequence.

We can mark the values $\tau(\overline{S})$ on the κ axis for different periodic orbits $\overline{S}$ and this gives a picture analog to the bifurcation tree in figure 1.3. In figure 1.16 a) we have marked the symbolic value of some periodic orbits orbits and in figure 1.16 b) we have also drawn some of the intervals that corresponds to stable windows in the smooth unimodal map. The κ-axis may be considered as a topologic or symbolic parameter axis. The ordering of bifurcations is the same along κ as along the parameter a and therefore are these two axis topological equivalent but the metric properties (scaling etc.) is different.

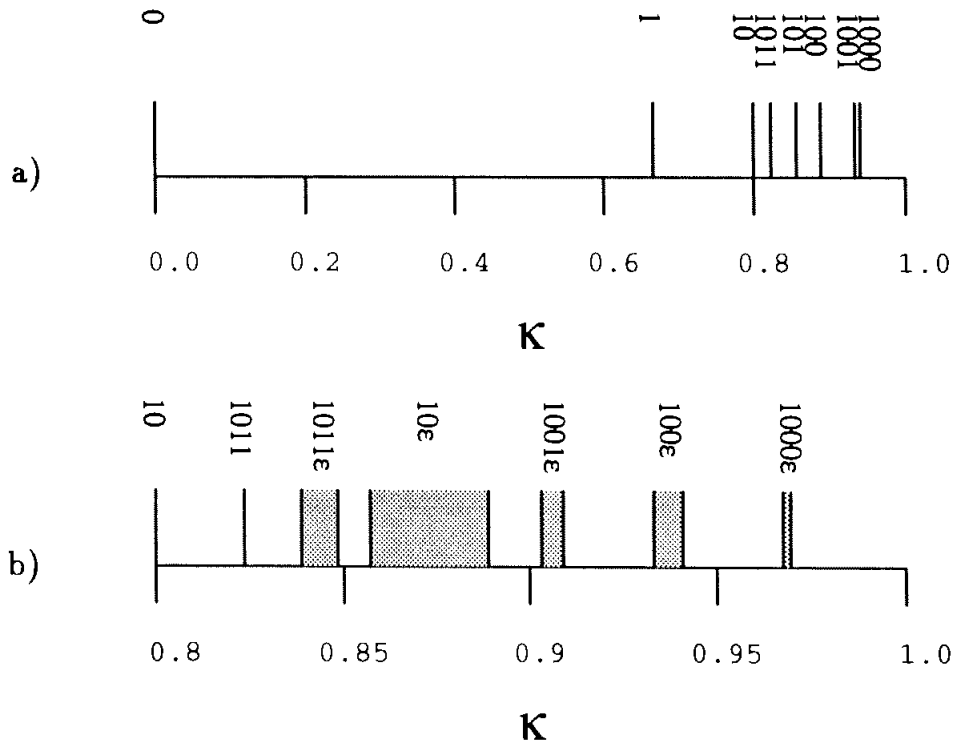

Figure 1.16: The bifurcation points of periodic orbits plotted at the symbolic parameter axis κ.

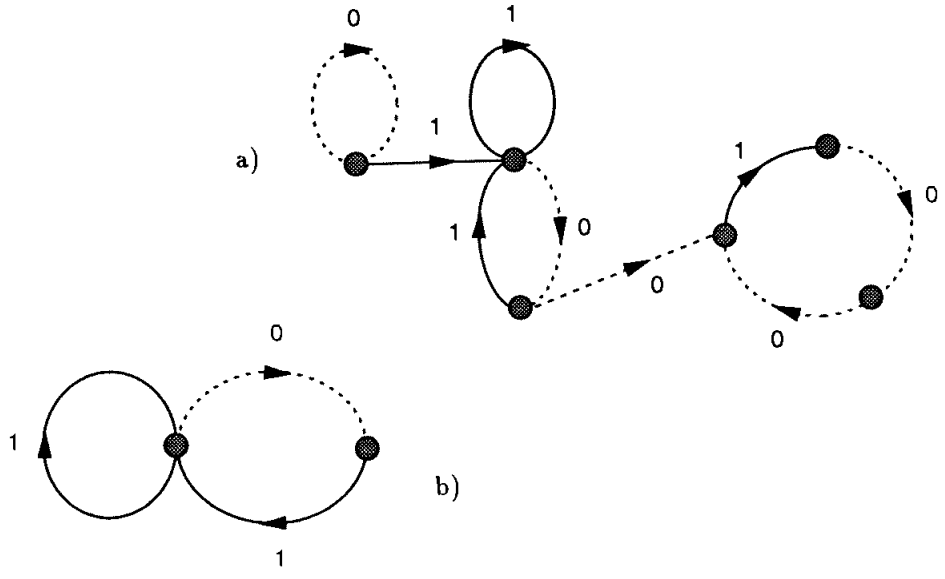

Figure 1.17: Graph representation of legal orbits for a parameter value that gives the stable period 3 orbit. a) The whole automaton. b) The Cantor set part of the automaton that follows after the 0–loop.

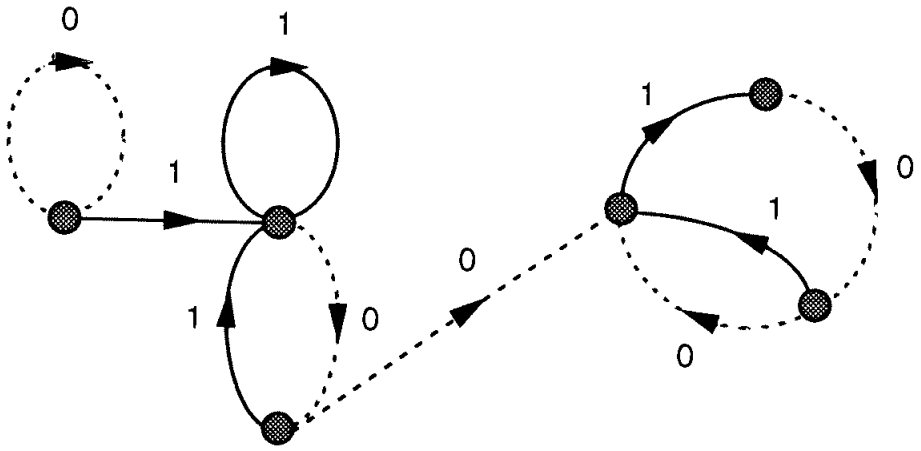

Figure 1.18: Graph representation of legal orbits for a parameter value that gives the crisis bifurcation of the period 3 resonance.

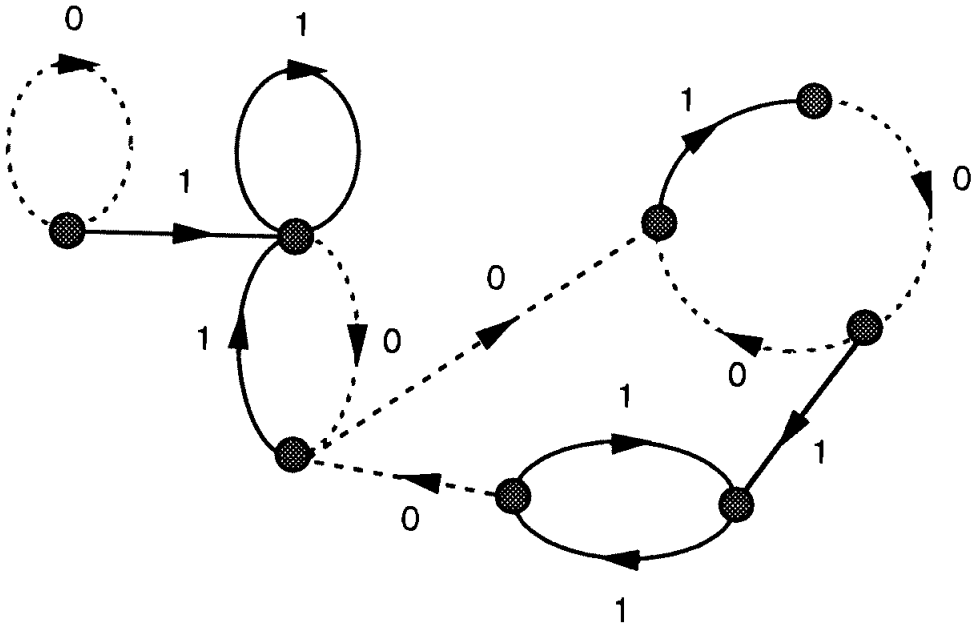

Figure 1.19: Graph representation for the kneading sequence $100101\overline{1}$.

The symbolic automaton graphs for the stable period 3 orbit $\overline{100}$ is drawn in figure 1.17 and the automaton at the band merging point is drawn in figure 1.18. In figure 1.17 a) the rightmost part of the graph is the stable orbit but of more interest is the middle part describing the fractal repellor. When removing the 0–loop to the left and the $\overline{100}$ attractor to the right, the remaining part is drawn in figure 1.17 b). This automaton gives the symbolic description of the Cantor set repellor consisting of all orbits created for a smaller parameter value except the isolated $\overline{0}$ fixed point. It can also be described by the alphabet

$$\{1, 01\} \tag{1.32}$$

The automaton for the kneading sequence $100\overline{101}$ in figure 1.19 shows that the fractal repellor $\{1, 01\}$ is still isolated and the attractor is the chaotic bands that can be described bye the alphabet

$$\{100, 101\} \tag{1.33}$$

with all combinations of symbols allowed. For any parameter value larger than the crisis bifurcation the $\{1, 01\}$ part is connected to the attractor giving one band attractor again. One example is given in figure 1.19 where the diagram for the kneading sequence $100101\overline{1}$ is drawn.

1.1.7 Resonances in the tent map

The tent map (1.3) has discontinuous $f'(x)$ and for $a > 1$ then $|f'(x)| = a > 1$ and there can not be a stable orbit as attractor. The fixed point $x_{\overline{0}} = 0$ is stable for $a < 1$ and unstable for $a > 1$. This does not prevent the map from having chaotic bands an in figure 1.4 we find that there are bands close to the bifurcation of the fixed point at $a = 1$ but no bands in a period 3 resonance or in any other resonance.

The band merging from $2n$ bands to n bands in figure 1.4 takes place when the slope of $f^{(2n)}(x)$ has absolute value 2. We have $|df^{(2n)}(x)/dx| = a^{2n}$ which gives a band merging for

$$a = 2^{\frac{1}{-2n}} \tag{1.34}$$

These values converges to $a = 1$ from above, not as a geometric series but much slower.

There exists no other band structure than the bands generated by the fixed point and a chaotic band has no internal resonance structure. This is easily shown because in the one band region $\sqrt{2} < a < 2$ the orbits of length n have slope $|df^{(2n)}(x)/dx| = a^{2n}$ and this is larger than 2 for all orbits $n \geq 2$ and then there are

no bands other than the period 1 band. The period 3 orbit is born, goes through all period doublings, band mergings and the crisis bifurcation at one singular parameter value $a = (1 + \sqrt{5})/2 = 1.6180\ldots$. This is one large jump in the plot of κ as a function of a in figure 1.13.

From the self similarity it follows that also the 2^n bands are without internal structure of bands. The slope is squared for each bifurcation and the shortest orbit born in the bands is twice as long and cannot have bands.

The plot of κ as a function of a in figure 1.13 has fewer steps and larger jumps for the tent map than for the logistic map because of the singular bifurcation points in the parameter a.

1.2 Construction of a finite automaton

There is a simple procedure giving the Markov graph or an automaton for the unimodal map when we know the kneading sequence K. We can also use the procedure to generate a Markov graph for other systems given a finite list of forbidden symbol strings.

In general there is no guarantee that the Markov graph for the unimodal map is finite. One example where the automaton is infinite is the accumulation point of the period doubling bifurcation [90]. If there exists a stable periodic orbit the automaton is finite and ends in a cycle with the symbols of the stable orbit. We may approximate the automaton for most parameter values with an automaton for a stable orbit at a parameter value close to the exact parameter value. We conjecture that the automaton converges to the correct automaton as we choose parameter values giving stable orbits closer and closer to the parameter value. The eigenvalue from the automatons converges to the limit also when the attractor is a chaotic orbit.

A different way to approximate the automaton is to approximate the kneading sequence by a string that after a finite number of symbols ends in a periodic orbit. This may be e.g. a band merging or a crisis bifurcations. This choice also gives a rational kneading value and a finite graph and we expect the eigenvalues will converge. The calculations are however more complicated and it is not so clear which part of the graph gives the largest eigenvalues.

The part of the automata which gives the eigenvalues we are interested in when there exist a stable orbit is a Cantor set repellor. We show how to find the topological entropy and other statistical measures from the automaton below. The repellor is the first loop structure that follows after the transient $\overline{0}$ loop and if they exist as

isolated transient loops, also after the $\overline{1}$ loop, $\overline{10}$ loop, $\overline{1011}$ loop, ... This is the period doubled loops of the fixed point. If the stable orbit is in the one-band region only $\overline{0}$ is a transient. If the stable orbit is in the two band region $\overline{0}$ is a transient followed by $\overline{1}$ as a transient and then followed by the repellor giving the largest eigenvalues. The four band region gives three transient loops etc.

One example is the stable orbit $\overline{100}$ in the one-band region for which the whole automaton is drawn in figure 1.17 a) while the Cantor set part is drawn in figure 1.17 b). We find in figure 1.18 that this Cantor set part is the same automaton also at the crisis bifurcation and it is the same graph all along the period 3 resonance.

The topological entropy (see section 1.3) for the transient repellor is here

$$h = \ln\left(\frac{2}{\sqrt{5}-1}\right) = \ln(1.618\ldots) \tag{1.35}$$

which is larger than the topological entropy for the three chaotic bands at the crisis bifurcation

$$h = \ln\left(2^{1/3}\right) = \ln(1.260\ldots). \tag{1.36}$$

The topological entropy for the chaotic bands at the crisis of a period n resonance is $1/n$-th of the topological entropy for the complete binary repellor $h = \ln 2$. The bands at the crisis of the period 3 resonance has the largest entropy in any resonance of the one band regime. The topological entropy at the band merging is given by the graph in figure 1.15 and gives $h = \ln\sqrt{2}$. The topological entropy is for the part of the graph following the 0 loop in the one band regime

$$\ln\sqrt{2} \leq h \leq \ln 2 \tag{1.37}$$

which is larger than any topological entropy in a resonance. By self similarity is the same true for the 2,4,8,...band regimes. We expect that the part of the Markov graph giving the largest topological entropy also gives the leading eigenvalues for other measures.

Since the repellor is constant from a tangent bifurcation to the crisis bifurcation we restrict ourself to choose stable periodic orbits born at a tangent bifurcation as other stable orbits inside a resonance do not give different leading eigenvalues.

The symbolic description of the possible orbits from a point x_0 in the unimodal map can be drawn as a path down a binary tree as drawn in figure 1.20. We refer to a node in the binary tree with the preceding symbol string and we refer to the top node as $\emptyset$. We first draw the kneading sequence $K = s_1 s_2 s_3 \ldots$ for the chosen parameter value as a path in the tree. From each node along this path there is a

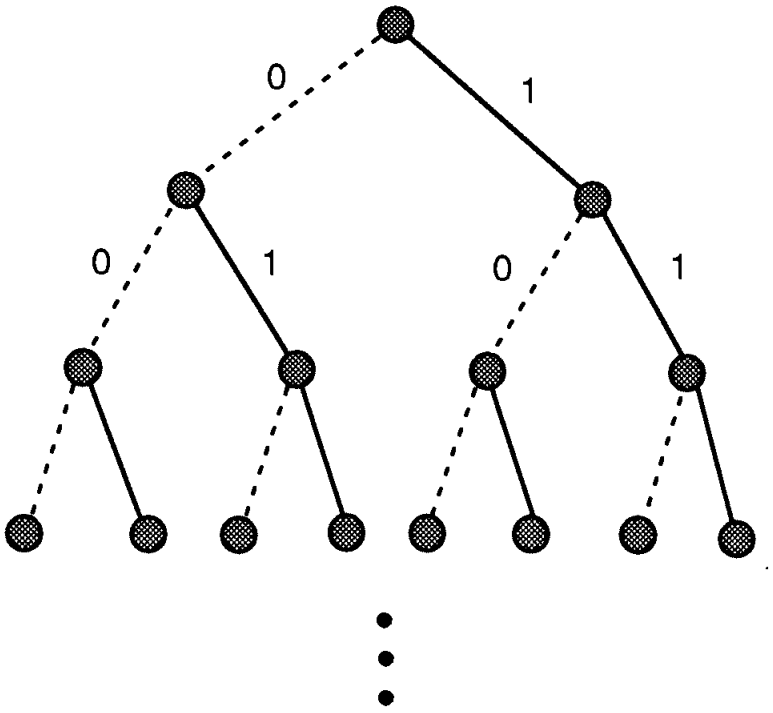

Figure 1.20: A binary tree.

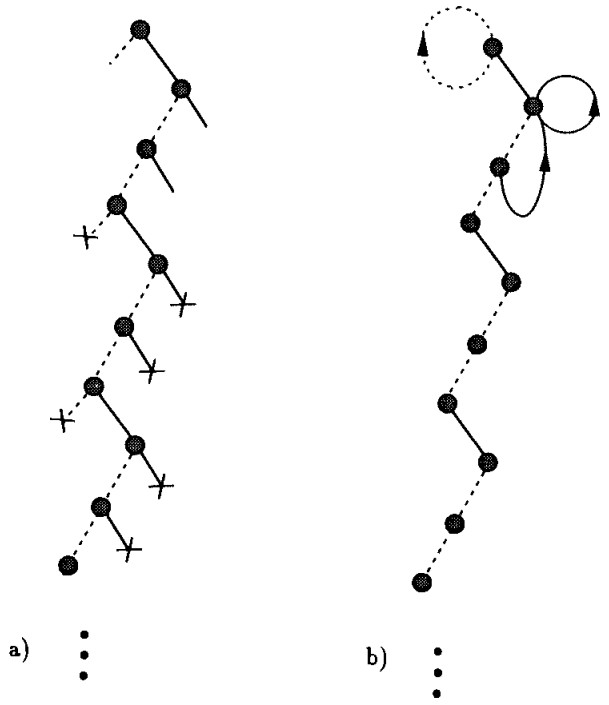

Figure 1.21: The construction of the stable period 3 automaton. In a) the forbidden side branches ends in a cross, and in b) the legal side branches are reconnected to the graph.

side branch and we have to decide if this is a legal branch. The side branch after the n–th node is $s_1 s_2 \ldots s_n(1 - s_{n+1})$ and this branch is legal if

$$\tau(s_i s_{i+1} \ldots s_n(1 - s_{n+1})) < \kappa \tag{1.38}$$

for all $i \in \{1, 2, \ldots n\}$. A side branch that is legal is connected to the node with the symbolic description $s_1 s_2 \ldots s_k$ where the symbol string is

$$s_1 s_2 \ldots s_k = s_{n-k+2} \ldots s_n(1 - s_{n+1}) \tag{1.39}$$

for the largest possible integer k. This procedure prevents that a legal side branch is followed by an illegal string. The automaton we obtain by this procedure can then be minimalized.

We give a few examples how to use this procedure. Figure 1.21 a) shows the path in the binary tree for the kneading sequence $K = \overline{100}$ with $\kappa = 0.\overline{111000}$. We

find the following legal side branches of the path

$$\begin{array}{rcllcl} 0 & \Rightarrow & \tau(0) & = 0 & < & \kappa \\ 11 & \Rightarrow & \tau(11) & = 0.10 & < & \kappa \\ 101 & \Rightarrow & \tau(101) & = 0.110 & < & \kappa \\ & & \tau(01) & = 0.01 & < & \kappa \\ & & \tau(1) & = 0.1 & < & \kappa \end{array}$$

and the forbidden branches

$$\begin{array}{rcllcl} 1000 & \Rightarrow & \tau(1000) & = 0.1111 & > & \kappa \\ 10011 & \Rightarrow & \tau(10011) & = 0.11101 & > & \kappa \\ 100101 & \Rightarrow & \tau(100101) & = 0.111001 & > & \kappa \\ 1001000 & \Rightarrow & \tau(1001000) & = 0.1110000 & < & \kappa \\ & & \tau(001000) & = 0.001111 & < & \kappa \\ & & \tau(01000) & = 0.01111 & < & \kappa \\ & & \tau(1000) & = 0.1111 & > & \kappa \\ & \vdots & & & & \end{array}$$

The forbidden side branches is marked by a cross in figure 1.21. The reconnection of the legal branches to a node following (1.39) gives

$$\begin{array}{rcl} 0 & \to & \emptyset \\ 11 & \to & 1 \\ 101 & \to & 1 \end{array}$$

and are drawn in figure 1.21 b). In figure 1.21 b) we see that the node 100100 has the same infinite future as the node 100 and we identify these two nodes and then we have the finite automaton of figure 1.17.

In figure 1.22 the construction of the automaton for the kneading sequence $K = 100101\overline{1}$ is shown.

These rules except the final reduction of the graph are implemented on a computer and given a stable periodic orbit by its symbolic string it gives the automata. On the computer the stable period n orbit loop is removed by letting also the string $s_1 s_2 \dots s_n$ be forbidden. This procedure for constructing a Markov graph is easily generalized to a construction of a n-ary tree where the forbidden strings are given as a finite list of strings. We than draw the paths of all forbidden strings in the tree. Then all side branches are checked, not by (1.38) but with the list of forbidden strings and the side branch is marked illegal if the string $s_i s_{i+1} \dots s_n(1 - s_{n+1})$, $i \in \{1, \dots, n\}$ is in the list. The reconnection of side branches is done by (1.39). A finite list of forbidden strings gives a finite automaton.

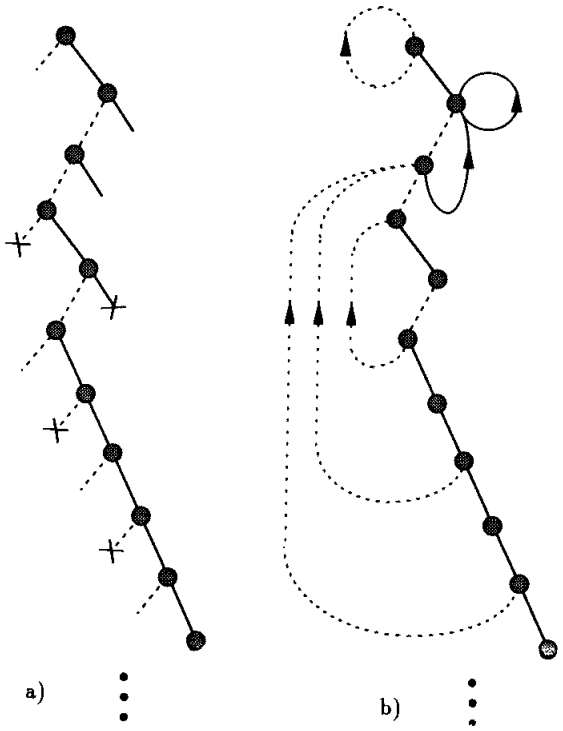

Figure 1.22: The construction of the automaton for kneading sequence $K = 100101\overline{1}$. In a) the forbidden side branches ends in a cross, and in b) the legal side branches are reconnected to the graph.

1.3 Topological entropy

The topological entropy h is a measure of the exponential growth of the number of periodic orbits with the length. This is the simplest of the average values one can find and it is the simplest application of the zeta-function formulation discussed in chapter 11 Let $N(n)$ be the number of periodic orbits of length n, then

$$N(n) \sim e^{hn} \tag{1.40}$$

in the limit $n \to \infty$. The number h can be obtained by calculating and counting periodic orbits, but if we know the symbolic description of the map h can be obtained in a much more effective way [45, 162, 40, 14].

The topological entropy is the negative logarithm of the leading (smallest and real) eigenvalue of the characteristic polynomial of the Markov matrix $h = -\ln z$. This polynomial

$$p(z) = 1 + a_1 z + a_2 z^2 + a_3 z^3 + \cdots = 0 \tag{1.41}$$

is obtained from the automaton by the following rules: a_i is initially 0; $a_i \to a_i - 1$ for each non self intersecting loop in the graph with i nodes; $a_i \to a_i \pm 1$ for each combination of non self intersecting loops that have no node in common and where the sum of the nodes is i. The sign $+$ is chosen when the number of loops in the combination is even and the sign $-$ if the number of loops is odd. This is applied for each part of the graph that is recursive; that is the part of the graph where one can get from any node in this part to any other node in the same part by some path. Each recursive part of the graph gives a eigenvalue and the smallest real eigenvalue gives the topological entropy.

$$h = -\ln z_0 \tag{1.42}$$

The simplest example is the complete binary map where the symbolic description of the repellor or the attractor is given by the automaton in figure 1.11. The automaton has two loops with length 1 and the loops can not be combined as they have one node in common. This give the polynomial

$$p(z) = 1 - 2z = 0$$

and from this $z = 1/2$ and

$$h = \ln 2$$

This result is of course easily obtained by just observe that since all combinations of the two symbols 0 and 1 are legal and most strings are not a repetition of shorter strings, then the number of periodic orbits grows as

$$N(n) \sim 2^n$$

The repellor in the period 3 resonance window in figure 1.17 b) gives one length 1 loop and one length 2 loop and topological entropy is then

$$\begin{aligned} 1 - z - z^2 &= 0 \\ z &= \frac{1+\sqrt{5}}{2} \\ h &= \ln\left(\frac{2}{1+\sqrt{5}}\right) \end{aligned}$$

A more interesting example is to choose a parameter value a that numerically gives a chaotic attractor and look at the convergence of h. If we choose $a = 3.8$ in the logistic map we find the kneading sequence

$$K = 10110111101101111010111101111 10\ldots$$

and we may e.g. find the automaton describing the repellor of the period 29 resonance close to the chaotic attractor. This gives a automaton with 29 nodes and the characteristic polynomial

$$\begin{aligned} p(z) \;=\; & 1 - z^1 - z^2 + z^3 - z^4 - z^5 + z^6 - z^7 + z^8 - z^9 - z^{10} \\ & + z^{11} - z^{12} - z^{13} + z^{14} - z^{15} + z^{16} - z^{17} - z^{18} + z^{19} + z^{20} \\ & - z^{21} + z^{22} - z^{23} + z^{24} + z^{25} - z^{26} + z^{27} - z^{28} \end{aligned}$$

and solving $p(z) = 0$ gives the smallest real root

$$z = 0.62616120\ldots$$

The error can be estimated to be of order $z^{29} \approx 10^{-6}$ because going from length 29 to a longer string typically for the unimodal map graphs or combination of loops with 29 and more nodes giving terms $\pm z^{29}$ and of higher order in the polynomial. Describing resonances of increasing length and with $a < 3.8$ we find polynomials with a better estimate for the topological entropy. For the closest stable period 90 orbit we find the topological entropy

$$\begin{aligned} h &= -\ln 0.62616130424685\ldots \\ &= \ln 1.59703257486152\ldots \\ &= 0.46814726655867\ldots. \end{aligned} \tag{1.43}$$

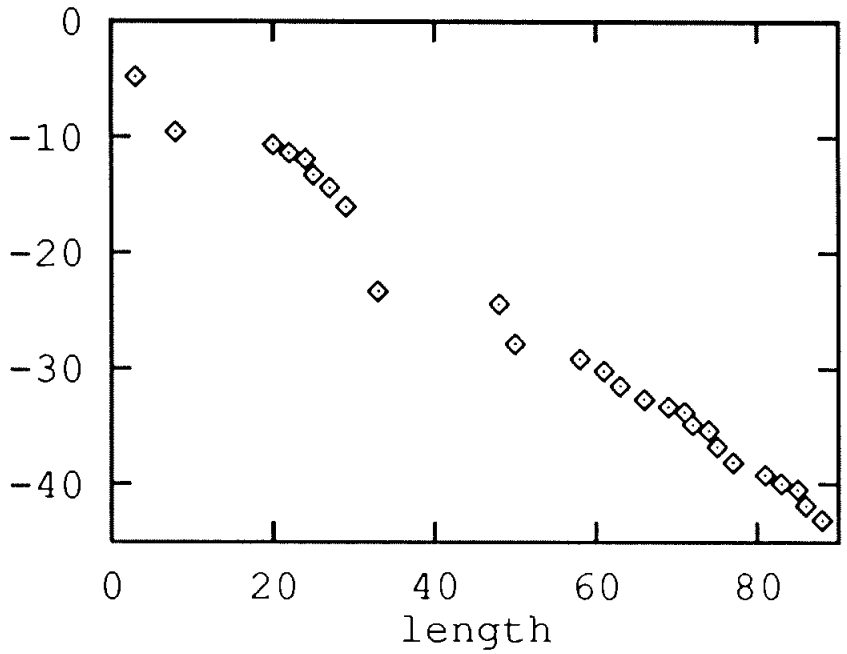

Figure 1.23: The logarithm of the difference between the leading zero of the characteristical polynomial and our best estimate as a function of the length for the logistic map $a = 3.8$.

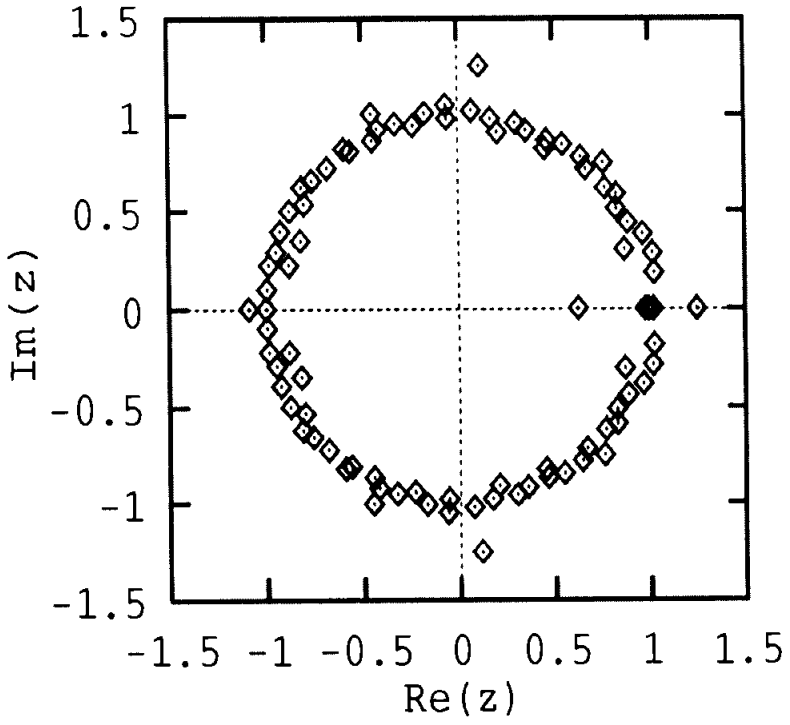

Figure 1.24: The zeroes of the characteristical polynomial for the logistic map $a = 3.8$ approximated up to length 90 symbolic strings.

We can find how fast this converges to our best estimate (1.43). In figure 1.23 is the logarithm of the difference between the zero of a polynomial and our best estimate plotted as a function of the length of the stable periodic orbit. The convergence is approximately linear with a slope of $-0.47 \approx h$.

We can find all real and complex zeroes of the characteristical polynomial and in figure 1.24 the zeroes of the polynomial obtained by including the forbidden strings of length 90 and less are plotted in the complex plane. The leading zero giving the topological entropy is the point closest to the origin while most of the other zeroes are close to the unit circle. This circle gives the radius of convergence.

All automatons for the unimodal map are simple because the automaton consists only of one long path of nodes and pointers back from a node to an earlier node.